Low-Noise, Single-Polarized, and High-Speed Vertical-Cavity Surface-Emitting Lasers for Very Short Reach Data Communication

Yen-Yu Huang[1], Yung-Hao Chang[1], Yaung-Cheng Zhao[1], Zuhaib Khan[1], Zohauddin Ahmad[1], Chia-Hung Lee[2], Jui-Sheng Chang[2], Cheng-Yi Liu[2], and Jin-Wei Shi[1*], *Senior Member IEEE*

Abstract- A novel technique is demonstrated for suppressing the relative intensity noise (RIN) and enhancing the high-speed transmission performance of 850 nm vertical-cavity surface emitting lasers (VCSELs). The orthogonal polarization suppression ratio (OPSR) of top-emitting high-speed 850 nm VCSELs with rectangular shaped mesas can be greatly enhanced by electroplating a copper substrate onto the backside, without any degradation in slope efficiency (output power). The enhancement of the OPSR results in a significant reduction of the RIN (around -130 vs. -145 dB/Hz) over a wide frequency range (near DC to 20 GHz) in comparison to the reference device without the additional copper substrate. Moreover, the structure of the demonstrated device can not only flatten the electrical-to-optical (E-O) responses but also narrow the spectral width due to the strain induced by the copper substrate. Overall, the lower RIN and flatter E-O frequency responses in turn lead to a significant improvement in the 25 Gbit/sec eye-opening and lower timing jitter in our demonstrated device.

Keywords: Semiconductor lasers, Vertical cavity surface emitting lasers, Fiber optics and optical communications

I. INTRODUCTION

The use of high-speed vertical-cavity surface-emitting lasers (VCSELs) operating around the 850 nm wavelength regime as light sources in multi-mode fiber (MMF) based communication channels has become mainstream in several applications, such as for very short-reach data communication [1-4], high-performance-computing (HPC) systems [1-4], and HDMI 2.1 or DisplayPort 2.0 cables [5]. However, complex modulation/de-modulation techniques, such as high level pulse-amplitude modulation (PAM) [6], orthogonal frequency-division multiplexing (OFDM) [7,8], and feed forward equalization (FFE) [5,9] are needed to boost the data rate per channel in the afore-mentioned systems, to alleviate the speed bottleneck encountered in 850 nm VCSELs under direct modulation. Clearly, needing to use such techniques to boost the data rate makes reducing the relative intensity noise (RIN) in the VCSEL even more critical.

Yen-Yu Huang[1], Yong-Hao Chang[1], Yaung-Cheng Zhao[1], Zuhaib Khan[1], Zohauddin Ahmad[1] and Jin-Wei Shi[1*], are with the [1]Department of Electrical Engineering, National Central University, Taoyuan 320, Taiwan, (e-mail*: jwshi@ee.ncu.edu.tw). Chia-Hung Lee[2], Jui-Sheng Chang[2] and Cheng-Yi Liu[2] are with Department of Chemical and Materials Engineering, National Central University, Zhongli, Taiwan

For example, in the case of 256GFC (28.9 Gbaud/lane) with a PAM4 modulation format, the required RIN must be lower than -135 dB/Hz [10]. Designing VCSELs that simultaneously offer high modulation speeds and very low RIN is thus very important to meet the requirements of the next generation of optical interconnect systems. A lower RIN in VCSELs can be realized by increasing the number of pairs of top p-type distributed Bragg reflector (DBR) mirrors, which leads to an increased photon lifetime (τ_p) inside the cavity. However, a larger τ_p usually decreases both the net E-O bandwidth and slope efficiency of the VCSEL [11,12]. Other effective ways to reduce the RIN can be realized by controlling the state of polarization of the VCSEL [13,14]. These methods include the growth of epi-layers on misoriented GaAs substrates [15], elliptical surface etching on the DBR layers [16], integration of the elliptic dielectric mode filter output [17], the utilization of asymmetric oxide apertures [18], and strain and gain anisotropy induced by metal stressor [19]. Among all the reported single-polarized VCSEL techniques, the implementation of a linear grating on the top DBR mirror is one of the most effective ways to obtain a large and stable orthogonal polarization suppression ratio (>20 dB) over the entire bias current range [20]. Nevertheless, the additional grating induced intra-cavity loss may reduce the τ_p and degrade the RIN performance. In this work, we demonstrate a novel approach to relax the fundamental trade-off between the modulation speed, RIN, and output power of high-speed VCSELs, through the application of a single polarized VCSEL structure with strain engineering. An electroplating process is performed to add an additional copper substrate to the backside of high-speed 850 nm VCSELs with rectangular and circular shaped mesas. The extra strain induced by the addition of the electroplated substrate acts to enhance the polarization suppression ratio without sacrificing the threshold current and slope efficiency (output power) [21]. This enhancement is accompanied by a narrowing of the spectral width and a significant reduction of the RIN (around -130 vs. -145 dB/Hz) over a wide frequency range (near DC to 20 GHz) as compared to those of the reference sample without the extra copper substrate. Moreover, the demonstrated VCSELs have flatter electrical-to-optical (E-O) frequency responses due to the strain induced enhancement of the hole mobility and the minimization of the influence of the carrier transport effect on the E-O bandwidth [22,23]. The superior RIN performance and flatter E-O responses of the demonstrated devices lead to lower timing jitter and improved 25 Gbit/sec transmission performance. The demonstrated device structure

This article has been accepted for publication in a future issue of this journal, but has not been fully edited. Content may change prior to final publication. Citation information: DOI 10.1109/JLT.2022.3151905, Journal of Lightwave Technology

offers a new way to further improve the eye-pattern (>56 Gbit/sec) quality of the next-generation of high-speed VCSELs under large-signal modulation.

II. DEVICE STRUCTURE AND FABRICATION

Figures 1 (a) and (b) show top views of the demonstrated VCSELs. Both devices had the same rectangular mesa structures but different long side orientations of <011> (for device A) and <01$\bar{1}$> (for device B). Devices A and B were both fabricated with three different active areas for comparison. Figures 2 (a) and (b) show conceptual cross-sectional views of our device (30×70 μm^2) along the short (AA') and long axis (BB'), respectively. Oxide-relief processes were performed to relax the RC-limited bandwidth [24,25]. The epi-layer structure which was grown in a molecular beam epitaxy (MBE) chamber (Intelligent Epitaxy Technology Inc.)[1] was composed of four compressively strained $In_{0.07}Ga_{0.93}As/Al_{0.3}Ga_{0.7}As$ MQWs sandwiched between 39-pair n-type and 24-pair p-type $Al_{0.93}Ga_{0.07}As/Al_{0.15}Ga_{0.85}As$ DBR layers with a single $Al_{0.98}Ga_{0.02}As$ layer (25 nm thickness) for oxidation. The VCSEL epi-layers were grown on a n$^+$ (001) GaAs substrate cut 2° off axis toward 111 which would lead to an intrinsically larger optical gain and polarized output light along the <01$\bar{1}$> orientation, as shown in Figure 2 [15]. Device fabrication started with mesa etching. Since the shape of the mesas is rectangular after wet etching, a rectangular shaped current-confined aperture can thus be expected after the wet oxidation process. As shown in Figure 2, for a 30×70 μm^2 mesa, the corresponding oxide aperture size is 5×45 μm^2. We thus expect most of the injected current induced optical gain to be along the long side of the mesa. For reference and benchmark comparison devices having circular mesas and circular oxide apertures (Wo) with a diameter as 9 μm were also fabricated. In this study, we intentionally aligned the low-gain (short; device A) or high-gain (long; device B) side of the mesa along the <01$\bar{1}$> orientation, where, as discussed above, the optical gain is intrinsically larger than in the other orientations. This was done to demonstrate the influence of our layout on the static and dynamic performance of the devices. After p-type contact metallization (Ti/Au; 50/200 nm), the device was passivated by the application of a SiO_2 layer (~300 nm). An ~3 μm thick polymethylglutarimide (PI) layer was then deposited for planarization. Finally, an ~2 μm thick Ti/Au layer was evaporated onto the topside of the chip to form metal pads for on-wafer probing. As illustrated in Figure 1, electroplating was performed to form n-metal contacts on the backside of the fabricated chips, which had 150 μm thick n$^+$ GaAs substrates (after lapping). By thinning the GaAs substrate from 500 to 150 μm we can expect influence of the strain induced by the backside electroplated copper substrate on the topside VCSEL device to be stronger. On the other hand, for the reference devices, lacking the electroplated copper substrate, we did not perform the substrate lapping process. Nevertheless, the roughness of GaAs substrate after lapping

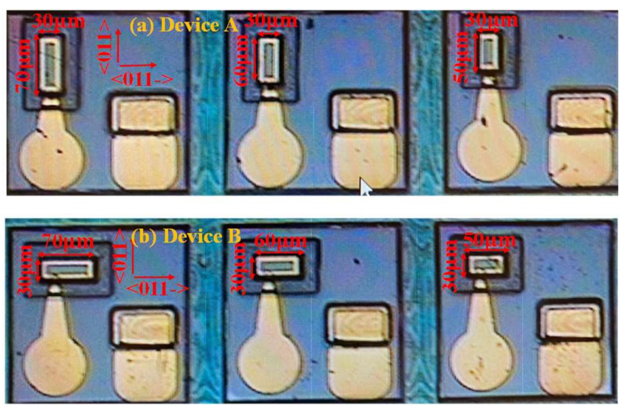

Figure 1. Top-views of the demonstrated VCSELs with long-side mesas along the (a) <011> orientation: device A and (b) <01$\bar{1}$> orientation: device B.

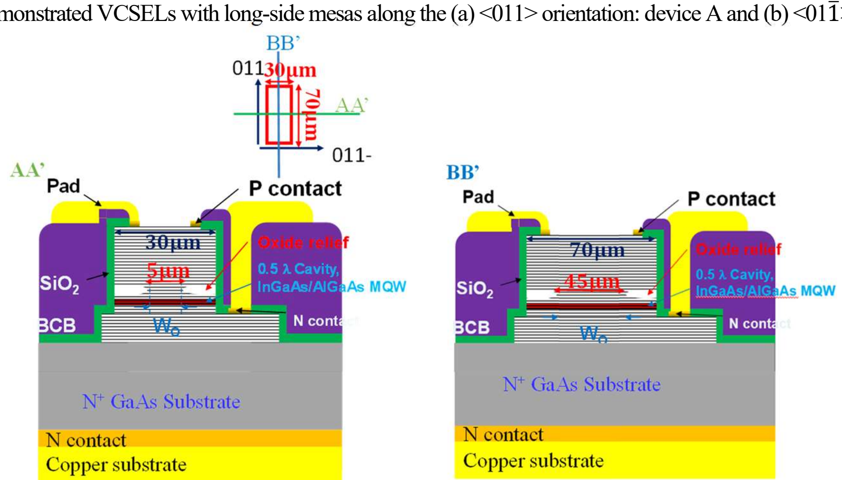

Figure 2. Conceptual cross-sectional views of the demonstrated VCSEL along the (a) short-side (AA' axis) and (b) long-side (BB' axis). For clarity, the figure is not drawn according to scale.

[1]Intelligent Epitaxy Technology, Inc. 1250 E Collins Blvd, Richardson, TX 75081, USA

This article has been accepted for publication in a future issue of this journal, but has not been fully edited. Content may change prior to final publication. Citation information: DOI 10.1109/JLT.2022.3151905, Journal of Lightwave Technology

should not be an issue affecting strain in the VCSEL. As in our previous works [21,26], the thinning of the substrate was the same for the reference devices as for the studied devices and the device with the electroplated copper substrates still exhibited significant improvements in static and dynamic performance. Here, the copper substrate was grown to around 100 μm in thickness. The strain induced by the composite substrates (GaAs and copper) has a significant influence on the dynamic and static performance of VCSEL devices, which will be discussed in greater detail later.

III. MEASUREMENT RESULTS

Figures 3 (a) and (b) show the measured L-I curves of devices A and B (before and after integration with electroplated copper substrate), respectively, in the two polarization states (<011> and <01$\bar{1}$>). The devices had the same active mesa size (30×70 μm^2). The polarization states of most of the reported VCSELs hop between two orthogonal orientations (<011> and <01$\bar{1}$>) with changes in the bias current [13,14]. Here, we define the measured optical power ratio in these two orientations as the OPSR, which can be obtained by using a polarizer during L-I curve measurement. A rotational arm connected to a well-calibrated optical sensor head with a polarizer mounted on its window was adopted for measurement. The orientation of this polarizer is rotated during measurement to extract the output power component in different polarization states. Using the same approach, we can also measure electroluminescence (EL) and μ-photoluminescence (PL) spectrum in different orientations using a polarizer [13] to further study the distribution of strain across the active mesa [27], linear gain anisotropy, as well as the birefringence [19] in the active MQWs layers. These will be included in future work. We can clearly see that each device exhibits strong polarized output light along the long (high-gain) side of the mesa after the electroplating process. In addition, in contrast to device B, which shows strong polarized light along the <01$\bar{1}$> orientation both before and after the electroplating process, device A only shows strong polarized light along the <011> orientation after the electroplating process. As discussed above, the epi-layers in our VCSEL are grown on a misoriented GaAs substrate (cut 2° off axis toward 111), which leads to a larger intrinsic optical gain and polarized output light along the <01$\bar{1}$> orientation [15]. However, in device A, the high current gain (long-) side follows the <011> orientation, which in turn leads to more balanced optical gains and output power in these two polarization states (<011> and <01$\bar{1}$>). Figure 4 shows the measured L-I curves and OPSR vs. bias currents of device A, before and after integration with the electroplated copper substrate. Figure 5 shows the same measurement results as in Figure 4 but for device B. To facilitate comparison of the change in the overall output power performance (slope efficiency; SE) of the VCSELs before and after the electroplating process, the optical power shown in these traces indicates the total output power from each device. Here, the OPSR of devices A and B is defined as the ratio of measured optical power in the orientations of <011> over <01$\bar{1}$> and <01$\bar{1}$> over <011>, respectively

The optical power values in these two main polarization states are obtained by installing an extra polarizer in the optical power sensor head during measurement, as illustrated in Figure 3. We can clearly see that after electroplating, there is a slight improvement in the SE of the L-I curves of both devices A and B, for the different mesa sizes. In addition, there are kinks in the L-I curves of some devices after electroplating process. These kinks can be attributed to the non-uniform carrier distribution induced non-uniform gain distribution within our long stripe light emission area [28], which may become more pronounced due to the influence of anisotropic external strain from the integrated copper substrate. Furthermore, due to such strain, both devices (A and B) show strong enhancement in the OPSR (up to over 15 dB in value). The SE for a semiconductor laser is determined by the internal loss (α_i) and mirror loss (α_m) [29]. The higher SE obtained for our device with the electroplated copper substrate can be attributed to the smaller α_i inside the cavity, where the free carrier (hole) absorption loss (α_{fc}) is usually the dominant term in the overall α_i. The α_{fc} is inversely proportional to the (hole) effective mass and free carrier (hole) mobility [30]. We can thus conclude that the smaller hole effective mass and the larger hole mobility in the electroplated VCSEL can effectively minimize the α_{fc} and α_i in the VCSEL cavity, which leads to the observed improvement in the SE. The enhancement in hole mobility of our electroplated VCSELs will be discussed in more detail later in relation to our dynamic measurement results. Both devices (A and B) exhibit very similar bias dependent output optical spectra. Figure 6 shows the measured L-I curves and OPSR vs. bias currents for the devices with circular apertures. We can clearly see that the enhancement in OPSR (<01$\bar{1}$> over <011>; <~2 dB) after electroplating process is not as significant as is the case with rectangular mesas due to the symmetry of the mesas and oxide apertures. Figure 7 shows the measurement results for device A before and after the electroplating process. We can clearly see that a narrowing of the spectral width occurs with the increase of length of the long-side of the mesa. This phenomenon can be attributed to the increase in the OPSR value with the length of the long side of the mesa, as illustrated in Figure 4. The single polarized light output with a high OPSR value leads to an increase of the selectivity of the fundamental lasing mode in the VCSEL [21,31], which results in the observed narrowing of the spectral width. Furthermore, there is a significant red shift (around 1 nm) in the central wavelength of device A after electroplating, which implies the occurrence of both compressive strain and thickening of the cavity layer in the longitudinal direction in our VCSEL structure. The degree of strain in our device can be directly measured by the double-crystal x-ray (DCXR) technique. In previous work, we have confirmed that the variation in the lattice constants (strain) as measured by DCXR before and after electroplating of the VCSEL is consistent with the results calculated from shifts in lasing wavelength and the ABCD matrix [21,29]. As can be seen in Figures 7 (b) and (e), there is a red shift of around 1.3 nm in the central wavelength (849.7 to 851 nm at 3 mA). In our simulation, the 1.3 nm shift in lasing wavelength corresponds to a 0.17 % increase in the lattice constant in the longitudinal direction (compressive strain).

This article has been accepted for publication in a future issue of this journal, but has not been fully edited. Content may change prior to final publication. Citation information: DOI 10.1109/JLT.2022.3151905, Journal of Lightwave Technology

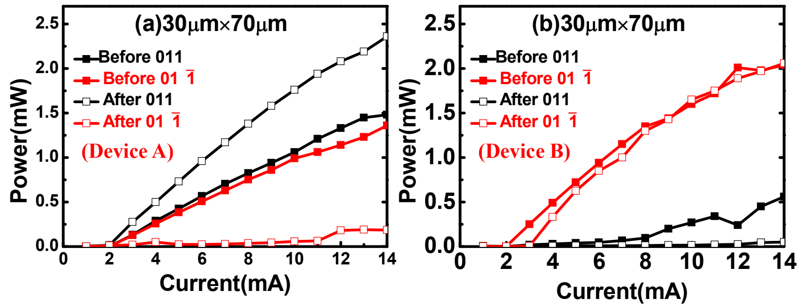

Figure 3. Measured L-I curves at <011> (black symbols) and <01$\bar{1}$> (red symbols) orientations of (a) Device A and (b) Device B before and after the electroplating process.

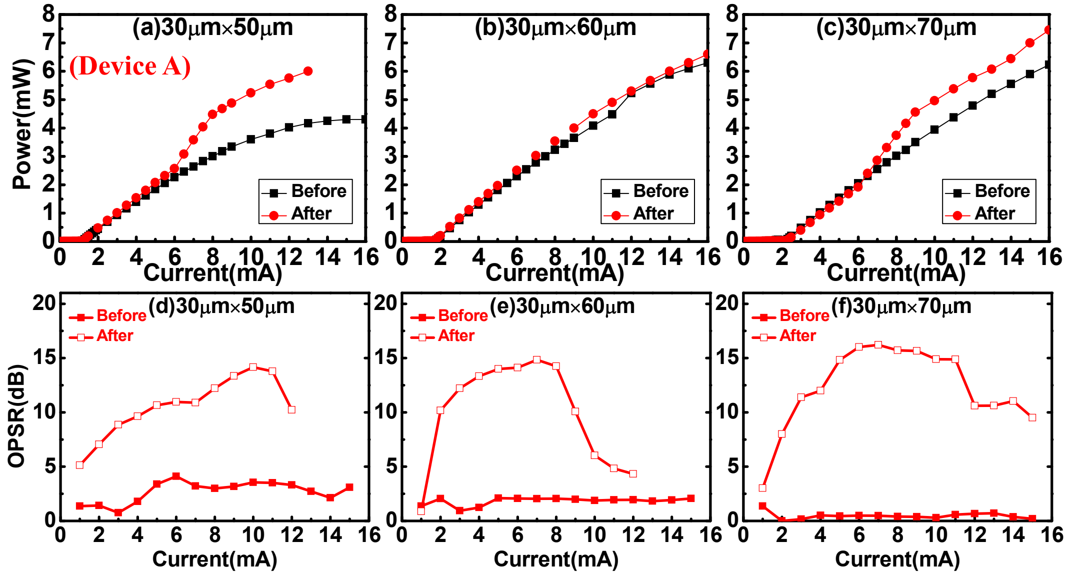

Figure 4. Measured L-I curves and OPSR values vs. bias currents of device A before and after electroplating for devices with three different active area sizes (a) 30×50, (b) 30×60, and (c) 30×70 μm^2

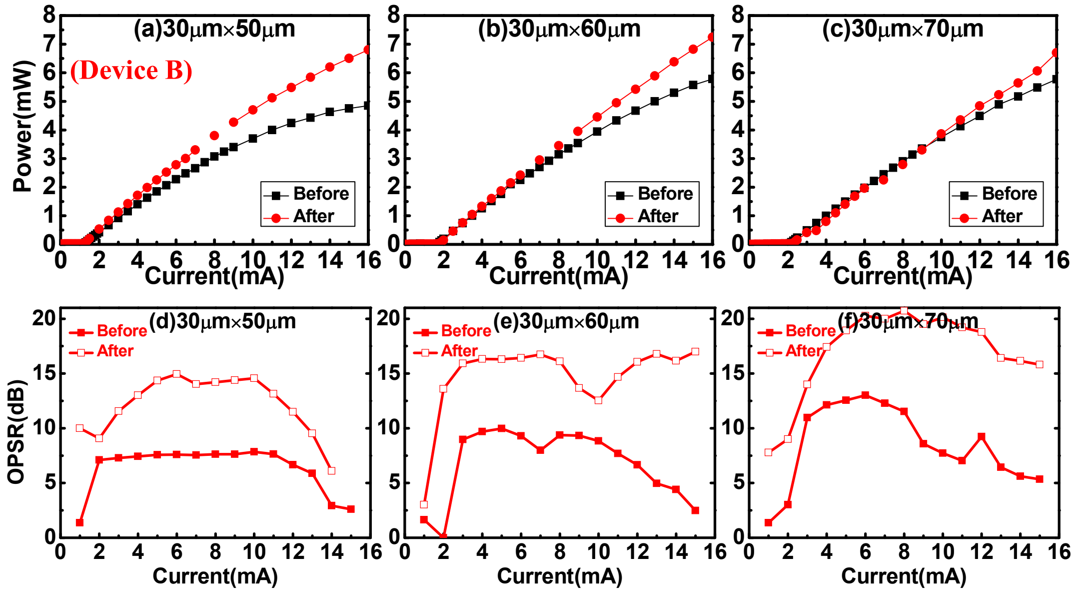

Figure 5. Measured L-I curves and OPSR values vs. bias currents of device B before and after electroplating for devices with three different active area sizes (a) 30×50, (b) 30×60, and (c) 30×70 μm^2.

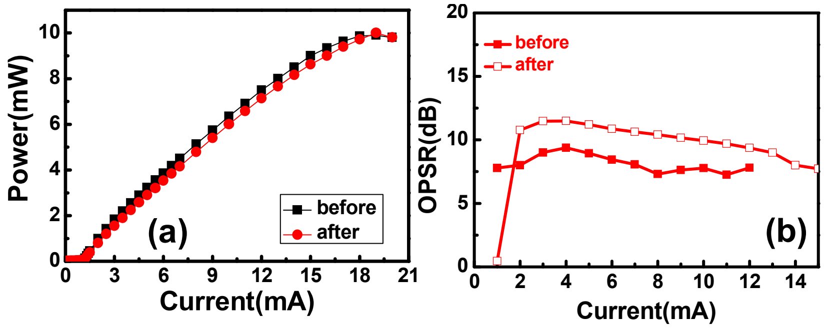

Figure 6. Measured (a) L-I curves (b) OPSR values vs. bias currents of device having circular W_o before and after electroplating process.

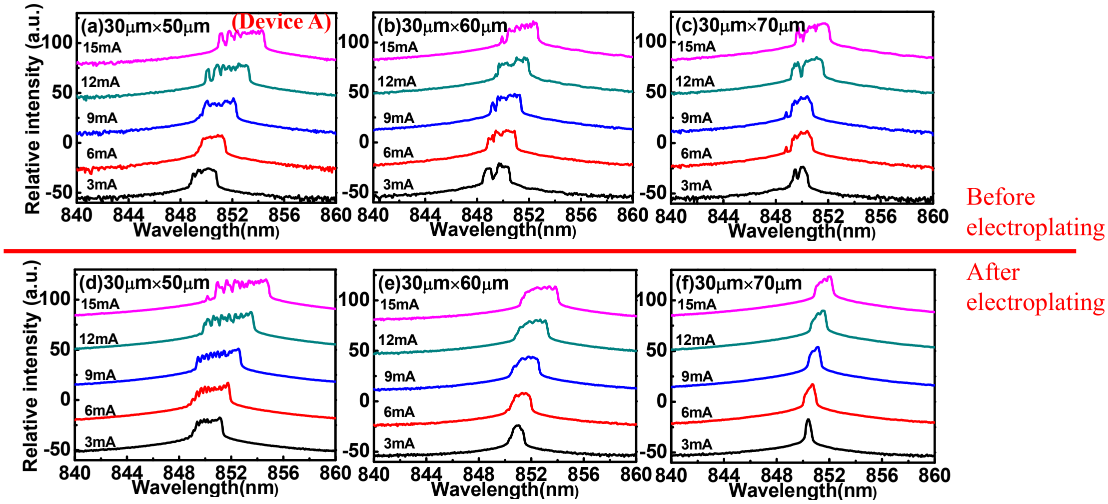

Figure 7. Measured bias dependent optical spectra of device A before and after electroplating for devices with three different active mesa sizes (a) 30×50, (b) 30×60, and (c) 30×70 μm^2.

On the other hand, for device B with the same mesa size (30×60 μm^2), the corresponding compressive strain is around 0.144 %. We can clearly see a minor difference in the compressive strain between these two axes (<01$\bar{1}$> and <011>). In addition, the obtained strain values are close to the numbers typical for compressive strain in the $In_xGa_{1-x}As/Al_xGa_{1-x}As$ MQWs of 850 nm VCSEL, which is usually less than 1% [31]. We may thus expect that the increased compressive strain inside the active MQWs ($In_{0.07}Ga_{0.93}As/Al_{0.3}Ga_{0.7}As$) induced by the additional electroplated copper substrate, will further deform the valence subband structure, leading to a smaller hole effective mass, and enhance the material gain [32,33]. More theoretical work is underway to calculate the external anisotropic strain induced gain enhancement and to compare this with the polarization dependent loss and other mechanisms that have been observed in our demonstrated devices [34]. Figures 8 and 9 show the measured bias dependent electrical-to-optical (E-O) frequency responses of devices A and B, respectively. The high-speed E-O performance of the fabricated devices was measured by a lightwave component analyzer (LCA), composed of a network analyzer (Anritsu 37397C) and a calibrated photoreceiver module (VI Systems: D50-1300 M)[2], capable of covering an optical window from wavelengths of 850 to 1310 nm. The measured O-E -3dB bandwidths for this photoreceiver module at wavelengths of 850 and 1310 nm are around 27 and 24 GHz, respectively. Here, the measured optical-to-electrical (O-E) frequency responses at 850 nm are selected for calibration during the de-embedding process for VCSEL E-O measurement. We can clearly see that there is a low-frequency roll-off (dip) at around 4 GHz in both devices before the electroplating process, but this is completely erased after electroplating. This kind of roll-off, commonly observed in the E-O responses of edge-emitting semiconductor lasers with a thick active layer [23] and single-mode VCSELs [35,36], can be attributed to the carrier transport effect. Compared with the traditional VCSEL with a circular oxide aperture [35,36], the hole transit time induced low-frequency roll-off is more pronounced in our case, because the rectangular shape of the mesa leads to a more significant hole transit time from the p-contact located on the short side of the mesa to the light-emission aperture. As can be seen in Figure 2, the effective aperture size for the case of a 30×70 μm^2 mesa, can be as large as 45 μm on the BB' axis, which in turn leads to a long transit time in the lateral direction. Nevertheless, the measured E-O frequency responses of both devices (A and B) show the elimination of low-frequency roll off after the addition of the copper substrate Such a significant improvement in the flatness of the E-O responses can be attributed to the enhancement of hole mobility (reduction of hole effective mass) and shortening of hole drift time in the InGaAs/AlGaAs based quantum wells under the influence of strain [33], which, in our

[2]VI Systems GmbH, Hardenbergstrasse 7, 10623 Berlin, Germany.

This article has been accepted for publication in a future issue of this journal, but has not been fully edited. Content may change prior to final publication. Citation information: DOI 10.1109/JLT.2022.3151905, Journal of Lightwave Technology

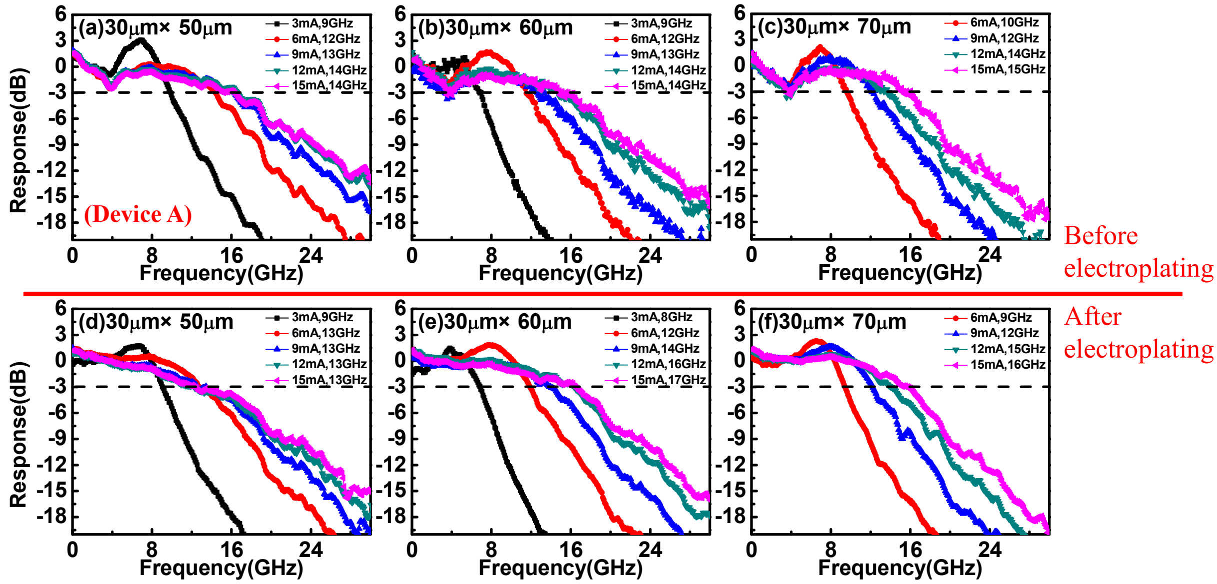

Figure 8. Measured bias dependent E-O frequency responses of device A before and after electroplating for devices with three different active mesa sizes: (a,d) 30×50, (b,e) 30×60, and (c,f) 30×70 μm^2.

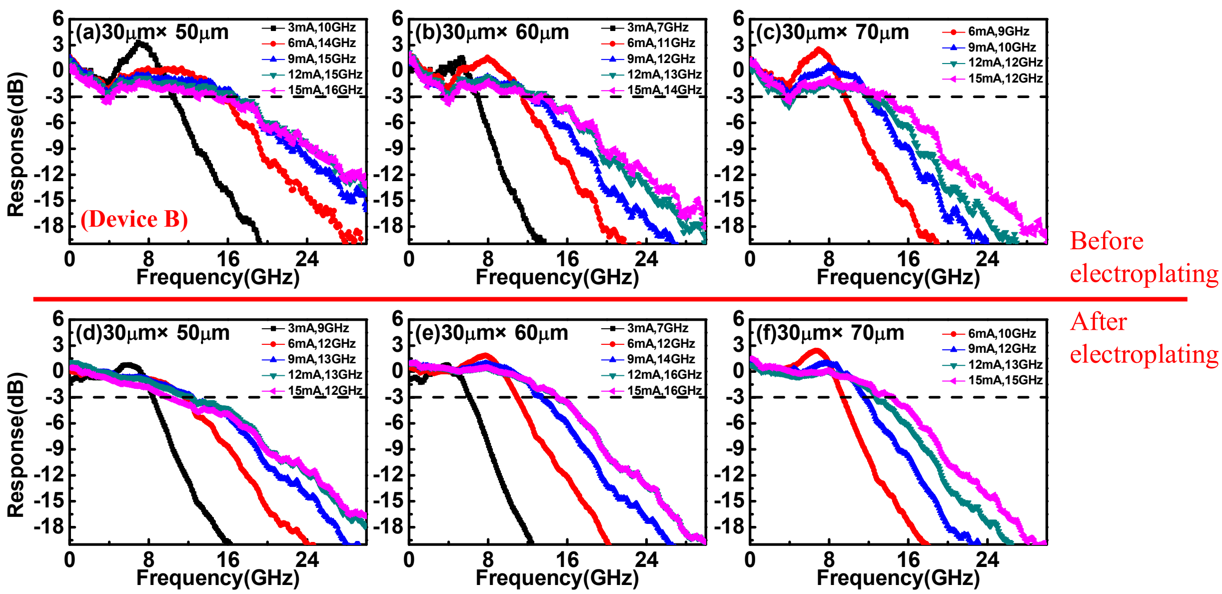

Figure 9. Measured bias dependent E-O frequency responses of device B before and after electroplating for devices with three different active mesa sizes (a, d) 30×50, (b, e) 30×60, and (c, f) 30×70 μm^2.

case, originates from the electroplated copper substrate. The measured bias dependent optical spectra and E-O frequency responses of reference device with the circular mesa structures are given in Figure 10. As can be seen, there is a significant red shift in the central wavelength with the rectangular mesas. Furthermore, the measured E-O frequency responses under high bias current (> 9mA) become flatter after the electroplating process due to the strain induced enhancement of the hole mobility, as discussed above. This phenomenon may be attributed to the lateral carrier transport effect becoming more pronounced in the VCSEL with the larger aperture size under a high bias current Overall, by combining the external strain induced by the addition of the electroplated copper substrate with the rectangular or circular shape of the mesa, our VCSELs can simultaneously achieve polarized light output with flat E-O responses. This implies a lower RIN noise [13,14] and a better quality of eye-opening under large signal modulation, which will be discussed later. The measured eye-patterns of device A are quite close to those of device B. Figures 11 to 13 show the measured 25 Gbit/sec eye-patterns of device B (before and after electroplating) for three different active mesa sizes, as specified on the figures. Here, we adopt the same optics setup as for the E-O bandwidth measurement but replace the high-speed photo-receiver module with a different one (VI Systems: R50-1300), comprised of a p-i-n photodiode and limiting amplifier with a 3-dB optical-to-electrical (O-E) bandwidth of around 30 GHz The O-E converted signal is then fed into a sampling scope to record and analyze the eye patterns.

This article has been accepted for publication in a future issue of this journal, but has not been fully edited. Content may change prior to final publication. Citation information: DOI 10.1109/JLT.2022.3151905, Journal of Lightwave Technology

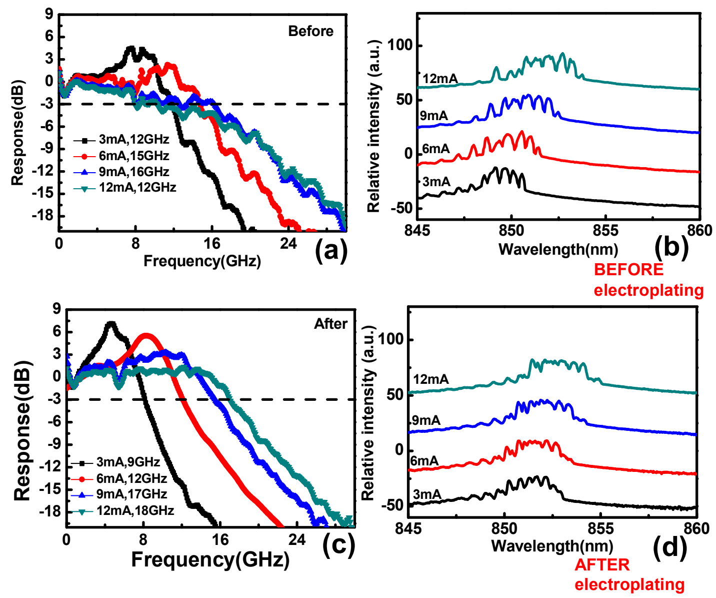

Figure 10. Measured bias dependent E-O frequency responses of devices with circular W_0 (a) before and (c) after electroplating process. Measured bias dependent optical spectra of the same devices (b) before and (d) after the electroplating process.

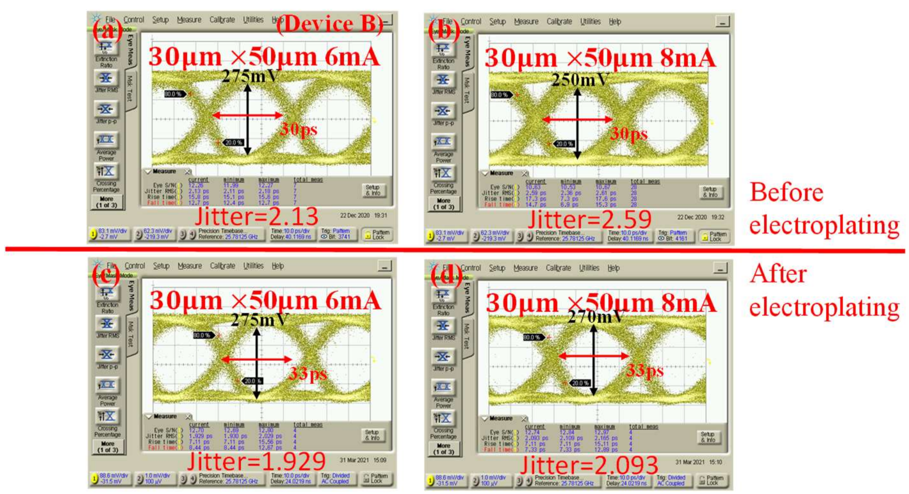

Figure 11. Measured 25 Gbit/sec eye patterns of device B under 6 and 8 mA bias currents and with a 30×50 μm^2 active mesa size before (a) - (b) and after (c) - (d) the electroplating process

A 25 Gbit/sec non-return-to-zero (NRZ) electrical signal with a pseudo-random binary sequence (PRBS) length of 2^{15}-1 is generated through a pattern generator to drive our VCSEL during testing. We can clearly see that there are significant improvements of eye-pattern quality in terms of smaller timing jitter in all devices measured after performing the electroplating process. Figure 14 shows the measured RIN spectra of device B before and after the electroplating process under the optimized bias currents for clear 25 Gbit/sec eye-opening. During measurement, the thermal noise is carefully de-embedded. The shot noise can be neglected because it is so small under the photocurrent (< 1 mA) typically used during measurement. For more detail about our RIN measurement setup please refer to [37]. As can be seen, the RIN of device B, with the electroplated copper substrate, is lower across a wide frequency range (near dc to 20 GHz) regardless of the studied device sizes. This can be attributed to the stronger polarized output light (larger OPSR) from device B than that from the reference devices without the electroplated copper substrate [13,14], as illustrated in Figures 3 to 5. The lower RIN and flattened E-O responses thus lead to the observed improvement in the 25 Gbit/sec eye-opening. The measured 25 Gbit/sec eye-opening and RIN noise performance of the reference device with circular mesas, before and after electroplating, are given in Figure 15 for comparison. We can observe that although the reduction in RIN after electroplating process is not as significant as that of the rectangular mesa device due to much smaller change in OPSR as illustrated in Figure 6, a great improvement in 25 Gbit/sec eye-opening can still be achieved. This occurs because of the flattening of the E-O response seen in Figure 10.

This article has been accepted for publication in a future issue of this journal, but has not been fully edited. Content may change prior to final publication. Citation information: DOI 10.1109/JLT.2022.3151905, Journal of Lightwave Technology

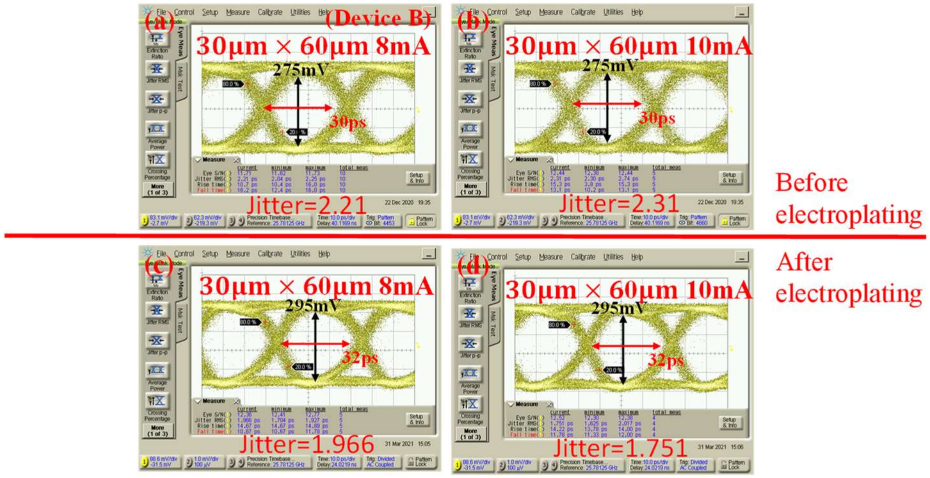

Figure 12. Measured 25 Gbit/sec eye patterns of device B under 8 and 10 mA bias currents and with a 30×60 μm^2 active mesa size before (a) - (b) and after (c) - (d) the electroplating process.

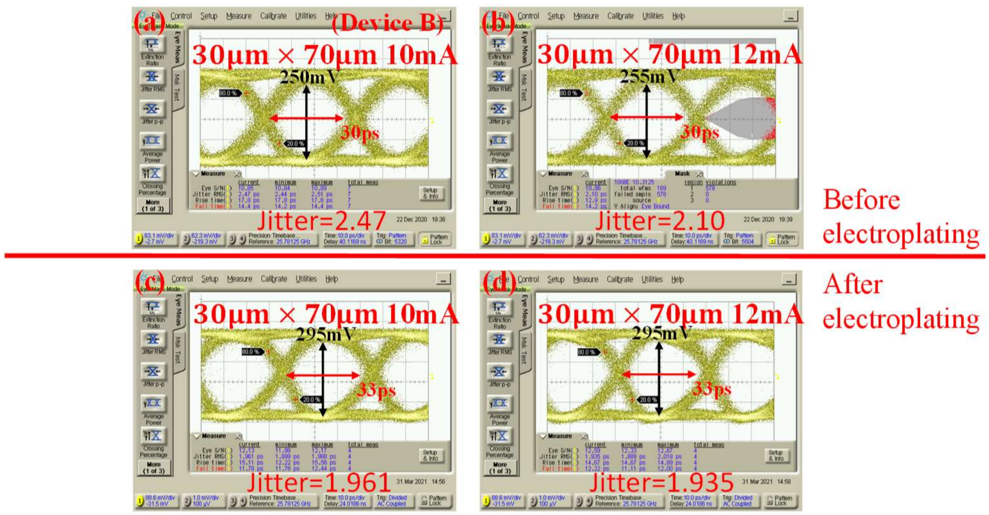

Figure 13. Measured 25 Gbit/sec eye patterns of device B under 10 and 12 mA bias currents and with a 30×70 μm^2 active mesa size before (a) - (b) and after (c) - (d) the electroplating process.

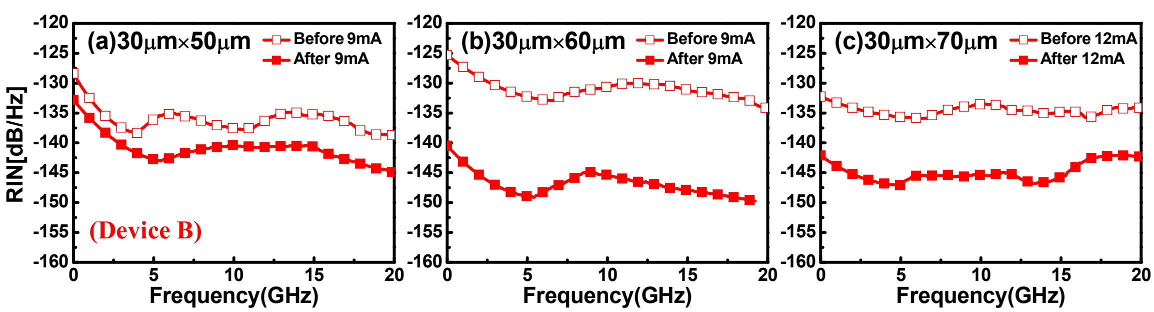

Figure 14. Measured RIN frequency responses of device B before and after electroplating for devices with three different active mesa sizes (a) 30×50, (b) 30×60, and (c) 30×70 μm^2. The bias current is optimized for clear eye-opening

This article has been accepted for publication in a future issue of this journal, but has not been fully edited. Content may change prior to final publication. Citation information: DOI 10.1109/JLT.2022.3151905, Journal of Lightwave Technology

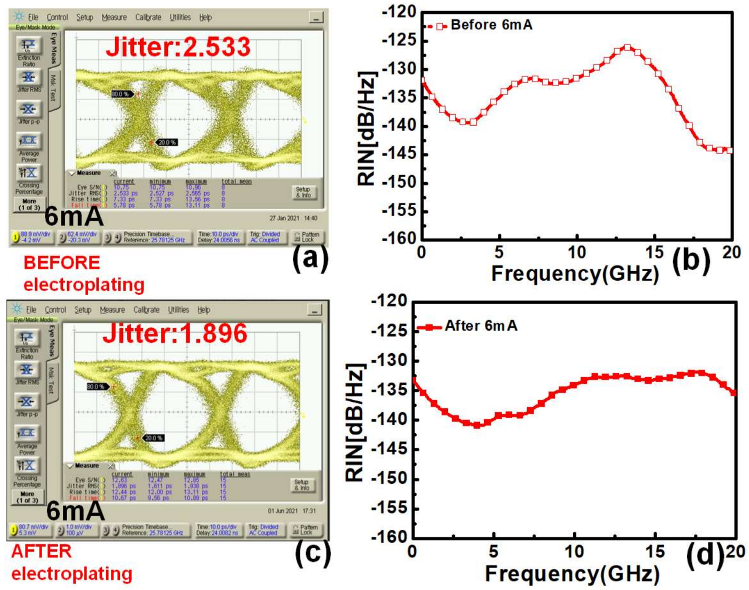

Figure 15. Measured 25 Gbit/sec eye patterns of devices with circular W_0 (a) before and (c) after electroplating process. Measured RIN frequency responses of the same devices (b) before and (d) after the electroplating process.

IV. CONCLUSION

A novel VCSEL structure for low RIN and high-speed performance with single polarized outputs is demonstrated. By combining a rectangular shaped mesa with an electroplated copper substrate in our VCSEL, significant enhancements of the OPSRs, narrowing of the spectral width, and reduction of the RIN over a wide frequency range (dc to 20 GHz) can be realized due to the external strain induced by the composite GaAs and copper substrates. Furthermore, this strain also leads to the increase of hole mobility in our GaAs based active layers, which minimizes the pronounced transit time limited E-O bandwidth in our device structure and greatly flattens the E-O frequency responses. Overall, as compared to those of reference devices without the additional copper substrate, the lower RIN and flattened E-O frequency responses of our demonstrated VCSELs result in significant improvement in 25 Gbit/sec eye-opening in terms of lower timing jitter, and larger eye-heights and widths.

ACKNOWLEDGMENTS

This research was funded by the Ministry of Science and Technology in Taiwan under grant number 110-2622-E-008-016. The authors would also like to thank the Intelli-EPI company for their assistance with the epitaxial layer growth

REFERENCES

[1] P. Moser, P. Wolf, G. Larisch, H. Li, J. A. Lott, and D. Bimberg, “Energy-efficient oxide-confined high-speed VCSELs for optical interconnects,” *Proc. SPIE,* vol. 9001, Feb. 2014, Art. no. 900103.

[2] E. Haglund, P. Westbergh, J.S. Gustavsson, E.P. Haglund, A. Larsson, M. Geen, and A. Joe, “30 GHz bandwidth 850 nm VCSEL with sub-100 fJ/bit energy dissipation at 25-50 Gbit/s,” *Electron. Lett*., vol.51, no. 14, pp. 1096-1098, Jul. 2015.

[3] D. M. Kuchta, A. V. Rylyakov, F. E. Doany, C. L. Schow, J. E. Proesel, C. W. Baks, P. Westbergh, J.S. Gustavsson, and A. Larsson, “A 71-Gb/s NRZ Modulated 850-nm VCSEL-Based Optical Link,” *IEEE Photon. Technol. Lett.,* vol. 27, no. 6, pp. 577-580, Mar. 2015.

[4] L. Chorchos, N. Ledentsov Jr., O. Makarov, P. Scholz, U. Hecht, C. Kottke, V. Jungnickel, R. Freund, V. A. Shchukin, V. P. Kalosha, J. P. Turkiewicz, F. Gerfers, N. Ledentsov, "NRZ, DB, and DMT performance for short-reach VCSEL-based optical interconnects," *Proc. SPIE,* vol. 11692, Mar. 2021, Art. no. 116920D.

[5] C. C. Kim, M. Kim, N. Kim, J. Pyo, J.- H. Je, "Direct optical-wire bonding: 3D writing of polymer-wire waveguides for optical interconnects," *Proc. SPIE,* vol. 11692, Mar. 2021, Art. no. 116920J.

[6] K. Szczerba, P. Westbergh, J. Karout, J. S. Gustavsson, Å. Haglund, M. Karlsson, P. A. Andrekson, E. Agrell, and A. Larsson, “4-PAM for High-Speed Short-Range Optical Communications,” *J. Opt. Comm. Netw.*, vol. 4, no. 11, pp. 885-894 , Nov. 2012.

[7] I.-C. Lu, C.-C. Wei*, H.-Yu Chen, K.-Z. Chen, C.-H. Huang, K.-L. Chi, J.-W. Shi*, F.-I. Lai, D.-H. Hsieh, H.-C. Kuo, Wei Lin, S.-W. Chiu, and J. (Jason) Chen, “Very High Bit-Rate Distance Product Using High-Power Single-Mode 850 nm VCSEL with Discrete Multi-Tone Modulation Formats Through OM4 Multi-Mode Fiber,” *IEEE J. of Sel. Topics in Quantum Electronics,* vol. 21, no. 6, Apr. 2015, Art. no. 1701009.

[8] R. Puerta *et al*., “107.5 Gb/s 850 nm multi- and single-mode VCSEL transmission over 10 and 100 m of multi-mode fiber,” presented at the Opt. Fiber Commun. Conf. Exhib., Mar. 2016, Paper Th5B.5.

[9] I-Cheng Lu *et al*., “Ultra Low Power VCSEL for 35-Gbps 500-m OM4 MMF Transmission Employing FFE/DFE Equalization for Optical Interconnects,” presented at the Opt. Fiber Commun. Conf. Exhib., Mar. 2013, Paper JTh2A.75.

[10] J. Petrila, “Scaling 128GFC,” https://standards.incits.org/apps/group_public/download.php/81212/15-332v0.pdf (incits.org)

[11] P. Westbergh, J. S. Gustavsson, B. Kögel, Å. Haglund, and A. Larsson, “Impact of Photon Lifetime on High-Speed VCSEL Performance,” *IEEE J.*

of Sel. Topics in Quantum Electronics, vol. 17, no. 6, pp. 1603-1613, Mar. 2011.
[12] D. M. Kuchta, J. Gamelin, J. D. Walker, J. Lin, K. Y. Lau, and J. S. Smith, “Relative intensity noise of vertical cavity surface emitting lasers,” *Appl. Phys. Lett*. vol. 62, no. 11, pp. 1194-1196, Dec. 1993.
[13] D. V. Kuksenkov, H. Temkin, and S. Swirhun, “Polarization instability and relative intensity noise in vertical-cavity surface-emitting lasers,” *Appl. Phys. Lett*, vol. 67, no. 15, pp. 2141-2143, Aug. 1995.
[14] T. Yoshikawa, T. Kawakami, H. Saito, H. Kosaka, M. Kajita, K. Kurihara, Y. Sugimoto, and K. Kasahara, "Polarization-controlled single-mode VCSEL," *IEEE Journal of Quantum Electronics,* vol. 34, no. 6, pp. 1009-1015, Jun. 1998.
[15] Y.-G. Ju, Y.-H. Lee, H.-K. Shin, and II Kim, “Strong polarization selectivity in 780-nm vertical-cavity surface-emitting lasers grown on misoriented substrates,” *Appl. Phys. Lett,* vol. 71, no. 6, pp. 741-743, Jun. 1997.
[16] P. Debernardi, H. J. Unold, J. Maehnss, R. Michalzik, Gian Paolo Bava and Karl Joachim Ebeling, "Single-mode, single-polarization VCSELs via elliptical surface etching: experiments and theory," *IEEE Journal of Selected Topics in Quantum Electronics,* vol. 9, no. 5, pp. 1394-1405, Oct. 2003.
[17] L. Xiang, X. Zhang, J.-W. Zhang, Y.-W Huang, W. Hofmann, Y.-Q- Ning, and L.-J. Wang, "VCSEL mode and polarization control by an elliptic dielectric mode filter," *Appl. Opt.*, vol. 57, no. 28, pp. 8467-8471, Oct. 2018.
[18] T. Aoki, R. Kubota, S. Yoshimoto, M. Yanagisawa, T. Ishizuka, and H. Shoji, "High-speed VCSEL arrays for 400 Gbit/s data center interconnects." *SEI Tech. Rev., vol.* 90, no. 71-75, Apr. 2020.
[19] Y. Matsui, D. Vakhshoori, P.Wang, P. Chen, C.-C Lu, M. Jiang, K. Knopp, S. Burroughs and P. Tayebati, "Complete polarization mode control of long-wavelength tunable vertical-cavity surface-emitting lasers over 65-nm tuning, up to 14-mW output power," *IEEE Journal of Quantum Electronics*, vol. 39, no. 9, pp. 1037-1048, Sept. 2003.
[20] E. Haglund, M. Jahed, J. S. Gustavsson, A. Larsson, J. Goyvaerts, R. Baets, G. Roelkens, M. Rensing, and P. O’Brien, "High-power single transverse and polarization mode VCSEL for silicon photonics integration," Opt. Express, vol. 27, no. 13, pp. 18892-18899, Jun. 2019.
[21] Jin-Wei Shi, Zuhaib Khan, Ray-Hua Horng, Hsiao-Yun Yeh, Chun-Kai Huang, Cheng-Yi Liu, Jie-Chen Shih, Yung-Hao Chang, Jia-Liang Yen, and Jinn-Kong Sheu, “High-power and single-mode VCSEL arrays with single-polarized outputs by using package-induced tensile strain,” *Optics Letters*, vol. 45, no. 17, pp. 4839-4842, Sep. 2020.
[22] A. Nainani, D. Kim, T. Krishnamohan and K. Saraswat, "Hole Mobility and Its Enhancement with Strain for Technologically Relevant III-V Semiconductors," *in Proceedings of International Conference on Simulation of Semiconductor Processes and Devices*, 2009, pp. 1-4.
[23] R. Nagarajan, T. Fukushima, S. W. Corzine, J. E. Bowers, "Effects of Carrier Transport on High Speed Quantum Well Lasers," *Appl. Phys. Lett.,* vol. 59, no. 15, pp. 1835-1837, Jul. 1991.
[24] Jin-Wei Shi, Jhih-Cheng Yan, Jhih-Min Wun, Jason (Jyehong) Chen, Ying-Jay Yang, “Oxide-Relief and Zn-Diffusion 850 nm Vertical-Cavity Surface-Emitting Lasers with Extremely Low Energy-to-Data-Rate Ratios for 40 Gbit/sec Operations,” *IEEE J. of Sel. Topics in Quantum Electronics,* vol. 19, no. 2, Apr. 2013, Art. no. 7900208.
[25] Jia-Liang Yen, Xin-Nan Chen, Kai-Lun Chi, Jason Chen, and Jin-Wei Shi, “850 nm Vertical-Cavity Surface-Emitting Laser Arrays with Enhanced High-Speed Transmission Performance Over a Standard Multimode Fiber,” *IEEE/OSA Journal of Lightwave Technology,* vol. 35, no. 15, pp. 3242-3249 Aug. 2017.
[26] Z. Khan, Y.-H. Chang, T.-L. Pan, Y.-C. Zhao, Y.-Y Huang, C.-H. Lee, J.-S. Chang, C.-Y. Liu, C.-Y. Lee, C.-Y. Fang and J.-W. Shi, “High-Brightness, High-Speed, and Low-Noise VCSEL Arrays for Optical Wireless Communication.” *IEEE Access*, doi: 10.1109/ACCESS.2021.3133436.
[27] M. Mokhtari, P. Pagnod-Rossiaux, C. Levallois, F. Laruelle, D. T. Cassidy, M. Bettiati, and J.-P. Landesman “Mechanical strain mapping of GaAs based VCSELs” *Appl. Phys. Lett,* vol. 118, pp.091102, 2021.
[28] Fang-I Lai, Ya-Hsien Chang, Li-Hong Laih, Hao-chung Kuo, and S. C. Wang "Improvement of kink characteristic of proton-implanted VCSEL with ITO overcoating", *Proc. SPIE*, vol. 5364, Jun. 2004, pp. 213-220.
[29] L. A. Coldren, S. W. Corzine, and M. L. Mašanović, “Mirrors and resonators for diode lasers,” in Diode Lasers and Photonic Integrated Circuits, L. A. Coldren, S. W. Corzine, and M. L. Mašanović, eds. (John Wiley & Sons, 2012), pp. 91-151.
[30] C. C. Chen, S. J. Liaw and Y. J. Yang, "Stable single-mode operation of an 850-nm VCSEL with a higher order mode absorber formed by shallow Zn diffusion," *IEEE Photonics Technology Letters*, vol. 13, no. 4, pp. 266-268 Apr. 2001.
[31] K.D. Choquette and R.E. Leibenguth, “Control of Vertical-Cavity Laser Polarization with Anisotropic Transverse Cavity Geometries” *IEEE Photonics Technology Letters,* vol. 6, no. 1, pp. 40-42, Jan. 1994.
[32] S. B. Healy *et al.*, "Active Region Design for High-Speed 850-nm VCSELs," *IEEE Journal of Quantum Electronics*, vol. 46, no. 4, pp. 506-512, Apr. 2010.
[33] S. W. Corzine, R.-H. Yan, L. A. Coldren, “Theoretical gain in strained InGaAs/AlGaAs quantum wells including valence-band mixing effects,” *Appl. Phys. Lett.,* vol. 57, pp. 2835-2837, Dec., 1990.
[34] K. Panajotov, B. Nagler, G. Verschaffelt, A. Georgievski, H. Thienpont, J. Danckaert and I. Veretennicoff, “Impact of in-plane anisotropic strain on the polarization behavior of vertical-cavity surface-emitting lasers,” *Appl. Phys. Lett,* vol. 77, no. 11, pp. 1590–1592, Jul. 2000.
[35] A. Haglund, J. S. Gustavsson, P. Modh, and A. Larsson, “Dynamic mode stability analysis of surface relief VCSELs under strong RF modulation,” *IEEE Photon. Technol. Lett.*, vol. 17, no. 8, pp. 1602-1604, Jul. 2005.
[36] J.-W. Shi, Z.-R. Wei, K.-L. Chi, J.-W. Jiang, J.-M. Wun, I.-C. Lu, J. (Jyehong) Chen, and Y.-J. Yang, “Single- Mode, High-Speed, and High-Power Vertical-Cavity Surface-Emitting Lasers at 850 nm for Short to Medium Reach (2 km) Optical Interconnects,” *IEEE/OSA J. of Lightwave Technol*., vol. 31, no. 24, pp. 4037-4044, Dec. 2013.
[37] S.- E. Hashemi, “Relative Intensity Noise (RIN) in High-Speed VCSELs for Short Reach Communication,” Master Thesis, Chalmers University of Technology, 2012.

Yen-Yu Huang’s biography is not available during paper submission.

Yung-Hao Chang was born in Tainan, Taiwan, on November 5, 1996. He received the graduate degree from the Department of Electrical Engineering, Yuan Ze University, Taoyuan City, Taiwan. He is currently working toward the master’s degree with the Department of Electrical Engineering, National Central University, Taoyuan, Taiwan. His current research interests high-speed and high-power VCSELs.

Yaung-Cheng Zhao was born in New Taipei, Taiwan, on October 29, 1996. He received the graduate degree from the Department of Electrical Engineering, National University of Kaohsiung, Kaohsiung City, Taiwan. He is currently working toward the master’s degree with the Department of Electrical Engineering, National Central University, Taoyuan, Taiwan. His current research interests high-speed and high-power VCSELs

Zuhaib Khan was born in Uttar Pradesh, India in 1992. He graduated from the Department of Electronics & Communication Engineering, Jamia Millia Islamia, New Delhi (India). He is currently pursuing his Ph.D. degree from Department of Electrical Engineering, National Central University at Taiwan. His current research interest includes High-speed, High Power VCSELs for application to Optical interconnects, 3D-sensing, Autonomous LIDAR and time of flight.

Zohauddin Ahmad was born in Bihar, India in 1989. He graduated from the Department of Nanoscience and Nanotechnology, Jamia Millia Islamia, New Delhi (India). He is currently pursuing a Ph.D. degree from the Department of Electrical Engineering, National Central University, Taiwan. His current research interests include high-speed modulator-based lasers, FMCW-Lidar and photonics integrated circuits.

Chia-Hung Lee's biography is not available during paper submission.

Jui-Sheng Chang's biography is not available during paper submission.

Cheng-Yi Liu was born in Hualien, Taiwan. He received the Ph.D. degree in materials science and engineering from the University of California, Los Angeles, USA, in 2000. He is currently a Professor with the Department of Chemical and Materials Engineering and the Director of the Optical Sciences Center, National Central University, Taoyuan City, Taiwan. His research interests include optoelectronic, micro-electro-mechanical systems, multilayer metallization process in semiconductor, and metal nanowire.

Jin-Wei Shi (SM'12) was born in Kaohsiung, Taiwan on January 22, 1976. He received his B.S. degree in Electrical Engineering from National Taiwan University, Taipei, Taiwan in 1998 and his Ph.D. from the Graduate Institute of Electro-Optical Engineering, National Taiwan University, Taipei, Taiwan in 2002. He was a visiting scholar at the University of California, Santa Barbara (UCSB), CA, in 2000 and 2001. In 2002-2003, he served as a post-doc at the Electronic Research & Service Organization (ERSO) of the Industrial Technology Research Institute (ITRI). In 2003, he joined the Department of Electrical Engineering, National Central University, Taoyuan, Taiwan, where he is now a professor. In 2011, he again joined the ECE Dept. of UCSB as a visiting scholar. His current research interests include ultra-high speed/power optoelectronic devices, such as photodetectors, electro-absorption modulators, sub-millimeter wave photonic transmitters, and semiconductor lasers. He has authored or co-authored more than 160 Journal papers, 160 conference papers and hold 20 patents. He was an invited speaker at the 2002 IEEE LEOS, 2005 SPIE Optics East, 2007 Asia-Pacific Microwave Photonic conference (AP-MWP), 2008 Asia Optical Fiber Communication & Optoelectronic Exposition & Conference (AOE), 2011 Optical Fiber Communication (OFC), and 2012 IEEE Photonic Conference (IPC). He served on the technical program committees for the OFC 2009-2011, 2012 SSDM, 2012 MWP, and 2013 Asia-Pacific CLEO. In 2007 he was the recipient of the Excellent Young Researcher Award from the Association of Chinese IEEE and in 2010 he received the Da-You Wu Memorial Award.